Trials of Pt-20%Rh versus Pt thermocouples between 157 °C and 962 °C

E Webster

Measurement Standards Laboratory of New Zealand, PO Box 31310 Lower Hutt 5040, New Zealand

E-mail: emile.webster@measurement.govt.nz

CrossMark

Abstract

For over a century the Type S (Pt-10%Rh) and R (Pt-13%Rh) thermocouples have been used as primary or secondary reference thermometers. However, the measurement uncertainties of both types at the silver point (~962 °C) are typically limited to about 0.5 °C, due to drift caused by crystallographic ordering between 200 °C and 500 °C and rhodium oxidation between 500 °C and 900 °C. Although both processes can be reversed using an 1100 °C anneal, regular annealing can be inconvenient or impracticable. This paper follows up a prior study indicating that an alternative noble-metal thermocouple comprised of Pt-20%Rh and Pt is relatively insensitive to both drift mechanisms. Four thermocouples, assembled using wire from four different manufacturers, were evaluated using a gradient-furnace and homogeneity scanner. Measurements were also made using a salt-bath (200 °C to 500 °C) and fixed points between the indium and silver points. The experiments indicate that individual thermocouples are stable at the silver point to within 0.18 °C for periods of up to 100 h and all four thermocouples have emf versus temperature characteristics within 0.3 °C of each other. This intrinsic stability and similarity, coupled with cost, assembly and use conditions identical to a Type R or S thermocouple make the Pt-20%Rh versus Pt thermocouple an attractive alternative. Recommended annealing procedures enabling the greatest stability are also given.

Keywords: reference thermocouple, rare-metal thermocouple, noble-metal thermocouple, platinum–rhodium thermocouple, homogeneity, thermoelectrical stability, thermocouple drift

(Some figures may appear in colour only in the online journal)

1. Introduction

Reference thermocouples continue to play an important role in many industrial and second-tier laboratories. These thermocouples are typically either the Type S (Pt-10%Rh/Pt) or Type R (Pt-13%Rh/Pt). Both of these thermocouple types have now been shown to suffer from reversible drift-inducing processes in the Pt–Rh alloy caused by either crystallographic ordering changes below 600 °C or by rhodium oxidation above 600 °C [1, 2]; the former cause an increase in the Seebeck effect and the latter causes a decrease. The changes in the emf caused by these two effects as a function of temperature, when homogeneity scanned at 100 °C, are illustrated in figure 1. The changes in Seebeck coefficient was induced by aging the thermocouple in a gradient furnace for 24 h and is described in more detail in section 2.3.1. Both ordering and oxidation changes are reversible and can be removed by using a >1 h 1100 °C anneal.

Although it is possible to make measurements with the Type S and R thermocouples with uncertainties ($k = 2$) lower than 0.1 °C [3], in practice, this is very difficult and requires high-quality thermocouples, which contain minimal irreversible inhomogeneities. These thermocouples must be regularly annealed and scanned to confirm a high level of homogeneity. The annealing step erases any reversible changes (ordering and oxidation) and ensures only irreversible inhomogeneities are present. Subsequent scanning then allows the correct quantification of reversible effects that unavoidably occur during most measurements. This onerous annealing and scanning processes must be frequently employed to minimise the inhomogeneity uncertainty component and reduce it to the lowest practicable level in the uncertainty budget. More
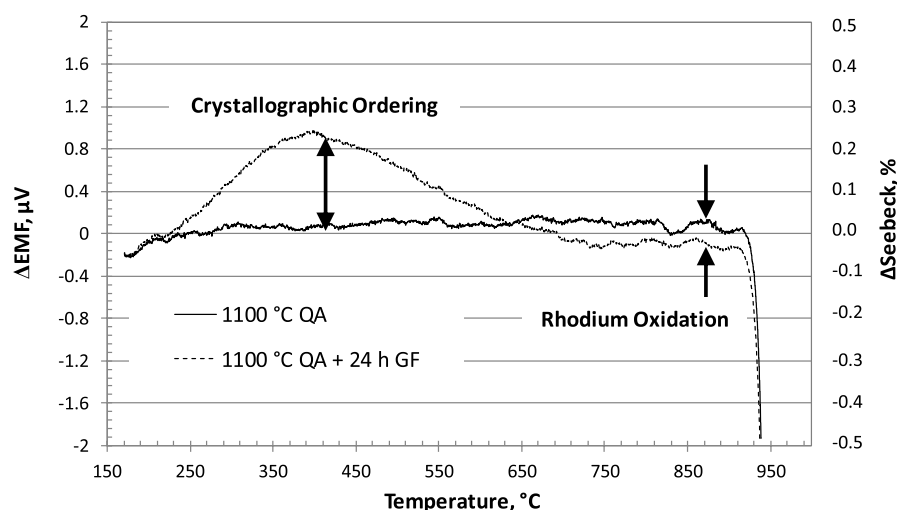
Figure 1. Typical changes in emf and Seebeck from an initial 1100 °C air quench anneal (QA) for a Type S thermocouple following a 24 h exposure to temperatures between approximately 170 °C and 950 °C in a gradient furnace (GF).

often, the inhomogeneity component for Types S and R is made using an educated guess derived from other studies or historic measurements. Consequently, in these situations, the uncertainty component is often too large to accommodate this guess work, ultimately restricting the total uncertainty ($k = 2$) to between 0.5 °C and 1 °C for temperatures <1100 °C.

For many users of these noble-metal thermocouples, it is impractical to apply regular anneals. The most common reasons for this are the permanent installation of the thermocouple, safety, the cost of loss of production incurred in shutting down a plant or process, or the lack of access to a suitable annealing furnace. Therefore, it would be desirable to find an intrinsically stable Pt/Rh thermocouple to alleviate annealing requirements and to lessen the uncertainty associated with drift caused by the formation of ordering and rhodium oxide. Although pure noble metals like Pt, Pd and Au are known to be far more stable, principally because they are immune to ordering effects and alloy composition changes, they are not always the most durable or reliable. For example, the large difference in expansion coefficient for dissimilar pure noble-metals makes them particularly prone to fatigue failures.

Some of the earliest research describing Pt-x%Rh/Pt thermocouples was by Caldwell and Acken [4, 5], early in the 20th century. Subsequent research was conducted by McLaren and Murdock in the 1980s [6]. This later work showed the Pt·20%Rh alloy to be more stable than other Pt-x%Rh alloys, but it was not actively pursued, possibly due to the well-established use of both the Type S and R thermocouples. More recently several NMI's (national metrology institutes) have shown a renewed interest in Pt-x%Rh thermocouple alloys [7–10], with the hope of finding more stable pairs for prolonged use at temperatures over 1100 °C, principally for high-temperature, high-value manufacturing processes. A recent study by Webster and Edler [2] investigated the temperature-induced drift characteristics of several Pt-x%Rh alloys at lower temperatures. This study revealed a distinct transition in both ordering and rhodium-oxidation behaviour at a Rh

concentration of 20%, in good agreement with McLaren and Murdock's work. Drift due to these two processes was seen to be largely absent in the Pt-20%Rh alloy.

In noble-metal thermocouples employing a pure Pt thermoelement (Types R, S, and the Pt/Pd) the Pt undergoes significant grain growth at temperatures over 1100 °C [11–13], leading to embrittlement and possible failure. The Pt thermoelement is also prone to contamination from rhodium-oxide vapour, causing a substantial reduction in the relative Seebeck coefficient [14–18]. Above about 1000 °C rhodium-oxide vapour, generated by the Pt-x%Rh thermoelement, can migrate both out of the alumina sheath and through microscopic cracks. It is for these reasons the potential of the Pt-20%Rh/Pt thermocouple is only explored up to 1100 °C, where the effects of Pt grain growth and Rh migration are minimal. For many users of reference thermocouples, this restricted temperature range is often sufficient for their needs.

This study investigates the performance of four Pt-20%Rh thermocouples assembled from wires from different suppliers to test the previous observations made using a single Pt-20%Rh sample [2]. It also aims to test the stability and drift signatures of these thermocouples after salt-bath and fixed-point measurements. Stability and drift are checked using homogeneity scans made in both the fixed-points and in a low-temperature high-accuracy homogeneity scanner. Lastly, a tentative reference function is suggested.

2. Experimental

2.1. Thermocouple samples

Four thermocouples were constructed using two assemblies to assess four Pt-20%Rh thermoelements from different suppliers. The first assembly, 20TC1, was made using a four-bore alumina sheath and the second, 20TC2, made using a twin-bore alumina sheath. The alumina insulators were both 1066 mm long with an external diameter of 4 mm. The bore size for 20TC1 was 0.8 mm diameter, whereas for 20TC2 it

Table 1. Description of thermocouples and thermoelements.

Pt/Rh thermoelement (diameter, mm)	Pt thermoelement (diameter, mm)	Insulator and (Pt/Rh supplier)	Supplied anneal state
80% Pt-20%Rh (0.5)	99.995 + % Pt (0.5)	20TC1 (FC)	Fully annealed
80% Pt-20%Rh (0.5)	99.995 + % Pt (0.5)	20TC1 (SC)	Fully annealed
80% Pt-20%Rh (0.5)	99.995 + % Pt (0.5)	20TC1 (GdFw)	As drawn
80% Pt-20%Rh (0.25)	99.995 + % Pt (0.5)	20TC2 (Alfa)	Fully annealed

FC: Franco Corradi, SC: Sigmund Cohn, GdFw: Good Fellow, Alfa: Alfa Aesar.

was 1.0 mm. Prior to use, the alumina insulators were baked at 1100 °C for 6 h to oxidise any potential contaminants. Both 20TC1 and 20TC2 used a single 0.5 mm diameter Pt wire from the same 10 m reel, having a purity greater than 99.995% (specified as reference grade). The four Pt-20%Rh wires were sourced from different suppliers. Three were of 0.5 mm diameter and one was of 0.25 mm diameter. By selecting a sample of smaller diameter, it was hoped that any surface-area-to-volume drift effects would be revealed. It is thought that smaller diameter wires are more susceptible to rhodium-oxidation, minor contaminants and grain growth failure [18, 19].

Before assembly, all thermoelements were first cleaned with alcohol followed by distilled water. The two Pt thermoelements were then carefully threaded into their respective alumina sheaths using a draw through technique [20, 21]. The four Pt-20%Rh thermoelements first required a high-temperature anneal to remove residual cold-work strain, produced during wire drawing and subsequent winding onto a bobbin. An electrical anneal at 1450 °C for 1 h was used for this purpose, after which the power was switched off, resulting in a rapid quench to ambient. Following the electrical anneal, the Pt-20%Rh thermoelements were also carefully drawn into their respective alumina insulators and a hydrogen gas welder used to join them to the corresponding Pt wire. After construction, the 20TC1 assembly contained three 0.5 mm Pt-20%Rh thermoelements and one 0.5 mm Pt thermoelement, and 20TC2 the single smaller diameter 0.25 mm Pt-20%Rh thermoelement and a 0.5 mm Pt thermoelement.

The final preparation step involved furnace annealing 20TC1 and 20TC2 for 2 h at 1100 °C, after which they were quickly withdrawn from the furnace and allowed to cool to room temperature (quench anneal, QA [22]). The QA leaves the thermocouples in a known and repeatable homogeneous base state. The main function of the QA is to remove reversible inhomogeneities and any minor cold-working caused by assembling the thermoelements into the insulators. The QA ensures that the subsequent formation of inhomogeneities are only those that cannot be avoided during normal use, namely through ordering and oxidation. Full details of the thermoelements are given in table 1. To limit drift from external sources, such as contamination, aging experiments were conducted in an additional closed-end 12 mm diameter quartz sheath. The sheath had been cleaned with alcohol and distilled water before being pre-baked at 1100 °C for 6 h.

2.2. Equipment

In the experiments that follow, a high resolution Keithley 2182A nanovoltmeter was used for all voltage measurements.

The homogeneity scanner employs a steam heat-pipe for the hot zone at ~100 °C and has an ambient temperature reference junction (cold zone), so does not require an ice-point. Only the emf resulting from the sharp temperature gradient of the scanner is needed to quantify the level of inhomogeneity [23]. However, for fixed-point measurements, an ice-point reference junction is necessary, for which an electronic ice-point (ISOTECH TRU 938/36) was used. Measurements were then made of the differences in emf between the electronic and a real ice-point, with the reference junction in the electronic ice-point and the hot-junction in the real ice-point. The corrections include any parasitic emfs generated by a shared noble-metal extension lead, which was used in all salt-bath and fixed-point measurements. All other equipment is that used in previous investigations of drift in thermocouples by this author [24].

2.3. Experimental methods

2.3.1. Gradient furnace aging. The core set of experiments followed the same procedure used in previous thermocouple drift studies [24]. Therefore, only a brief description is given here for the gradient-furnace, homogeneity scanner and the aging sequence. After an initial QA, the thermocouples were placed in the linear gradient-furnace with the hot junction at a location corresponding to 950 °C. The linear region within the gradient furnace spans 70 °C and 1100 °C, over a 1 m length with a standard deviation of 1.5 °C relative to the linear ideal. The resulting temperature gradient is therefore, approximately 0.9 °C mm^{-1}. Within the gradient-furnace thermocouples are simultaneously exposed to all temperatures in the linear range, up to a maximum determined by the thermocouples length (950 °C). At time periods of 1 h, 4 h, 24 h and 100 h the thermocouples were rapidly removed from the gradient-furnace and allowed to cool naturally to room temperature, quenching in any metallurgical changes. After cooling, the thermocouples were scanned in the homogeneity scanner. The scanner has a spatial resolution of about ±5 mm, which, when combined with the temperature non-linearity of the gradient-furnace, results in a temperature resolution of around ±5 °C. Changes in Seebeck coefficient caused by temperatures in the gradient-furnace can be correlated with position along the length of the thermocouple, and therefore temperature of exposure, to within ±5 °C. The combination of gradient-furnace and scanner enables the direct measurement of the temperature- and time-dependence of changes in the Seebeck coefficient (see, for example, figure 1).

2.3.2. Salt-bath and fixed-point experiments. Measurement comparisons between a calibrated SPRT and the four thermo-

couples were made in a salt-bath (Hart 6055) between 200 °C and 500 °C at 50 °C intervals. The expanded uncertainty in temperature at each of the set-points was less than 5 mK. The purpose of these measurements is to supplement those made at the fixed-points and allow for a greater density of data points when the reference function is generated.

Measurements with the four thermocouples were also made at the silver (Ag), aluminium (Al), zinc (Zn), tin (Sn) and indium (In) fixed-points, starting at Ag and ending at In. After the Ag and Al measurement, the homogeneity of each thermoelement pair was checked using the homogeneity scanner. A linear slide fastened atop each fixed-point furnace also allowed the immersion profiles to be assessed both continuously and at fixed immersions for each of the Pt-20%Rh thermoelements. The immersion profiles will be the resulting convolution of the fixed-point thermal gradient and any thermal signatures that evolve during the measurement, so are of limited use for determining inhomogeneity. However, the immersion scan can reveal potential conduction errors. Undesirably, there is poor thermal connection between the thermocouple and the freezing metal within the cell, mostly due to the many layers of insulation (two of quartz and one of graphite). Therefore, the immersion profile was measured at increments of 10 mm over 100 mm with pauses of two minutes between measurements to allow thermal equilibration.

3. Results and discussion

3.1. Gradient furnace aging between 170 °C and 950 °C

Figures 2–5 show respectively the changes in emf that occurred in the four Pt-20%Rh thermoelements as a function of time and temperature, when measured between 20 °C and 100 °C (ΔT of 80 °C) in the homogeneity scanner. To enable comparison of the results they are presented as a difference in emf (Δemf) between the mean emf following an 1100 °C quench anneal (emf_{QA}) and after each gradient furnace exposure (emf_{Aged}),

$$\Delta emf = emf_{QA} - emf_{Aged}. \tag{1}$$

The solid black line represents the initial 1100 °C quench anneal (QA) state and the dashed black line (mostly lying atop the solid black line) the final QA state, applied at the end of the aging experiments. The almost imperceptible difference between the two QA scans demonstrates the highly repeatable homogeneous state that can be achieved through careful annealing. It should be noted, the Seebeck coefficient for the Pt-20%Rh versus Pt thermocouple is comparable to the Type S at the indium-point, but steadily exceeds that of the Type S and R as the temperature is increased, being roughly 20% higher at the silver-point.

As was seen in the earlier study [2], there is almost no change in the Pt-20%Rh thermoelements below 650 °C. However, above 650 °C there is a small increase in the emf as a function of temperature and time, with slight differences between all four Pt-20%Rh thermoelements. The Alfa 0.25 mm diameter wire sample appeared no less stable than the 0.5 mm samples, even after 100 h of aging, and perhaps

showed signs of greater stability when compared to the other three. Despite all four thermocouples showing some drift, it is still substantially less than has been observed in either a Type R or S [1, 25]; see for example figure 1, which is plotted on the same scale as figures 2–5. Further comparisons with Type R and S are explored in more detail in section 3.2. The most probable causes of the changes are either crystallographic reordering effects or Rh depletion due to oxidation.

A scanning electron microscope showed that the Pt-20%Rh alloy developed a thick coating of rhodium oxide at 800 °C in air. The rhodium oxide was seen to form mostly at the grain boundaries and to a lesser extent on the grain surfaces. This oxide started forming at about 600 °C and reached a maximum thickness between 800 °C and 900 °C. As the temperature was increased beyond 900 °C a complex disassociation process started occurring, with progressively more of the oxide being reduced back into solid metal, and by 1000 °C the transformation was almost complete. Alloys with lower concentrations of Rh tended to only form rhodium oxide at the grain boundaries. These results are in good agreement with other studies on rhodium oxidation [15, 26, 27].

Lattice reordering, although possible, seems an unlikely cause for the observed changes in figures 2–5. Above 650 °C, the thermal energies involved are more likely to destroy ordered structures rather than create them [21]. Close analogies can be made with studies on the Type K thermocouple, specifically the ones focusing on the MIMS format [28, 29], in which no oxidation processes were present in the results. In both Type K (Ni-Cr leg) and Type S (Pt–Rh leg) it has been shown that ordered structures are progressively removed with increases in temperature beyond approximately 450 °C [1, 22, 28]. Further evidence for rhodium oxidation being the cause of changes in emf can be made using Caldwell's data [4], which shows that the expected change in emf due to a small reduction in Rh content (Pt-20%Rh), when measured at 100 °C, will result in an increase in emf. This topic is discussed in more detail in section 3.2. Therefore, oxidation leading to Rh depletion is the more probable cause of changes in homogeneity.

3.2. Variations in emf due to minor changes in Rh concentration

It is generally accepted that the formation of Rhodium-oxide causes a small reduction in the Rh concentration for Pt–Rh thermocouples, resulting in changes to the emf [15, 26]. For Types S and R these changes in Rh concentration have been found to scale well with temperature and lead to a reduction in emf at all temperatures [30]. This behaviour is best illustrated using Caldwell's data [4], which has been reproduced in figure 6(a). It can be seen from a dotted line drawn upward at the 10% Rh point that any reduction in Rh will cause a corresponding reduction in the emf, becoming larger as the temperature increases. The result for a similar dotted line drawn at 20% Rh concentration is quite different; most notably the changes in emf with temperature and Rh content are far small than in Types S and R, but also the effect changes sign at ~300 °C. Below this temperature a reduction in Rh content causes a slight
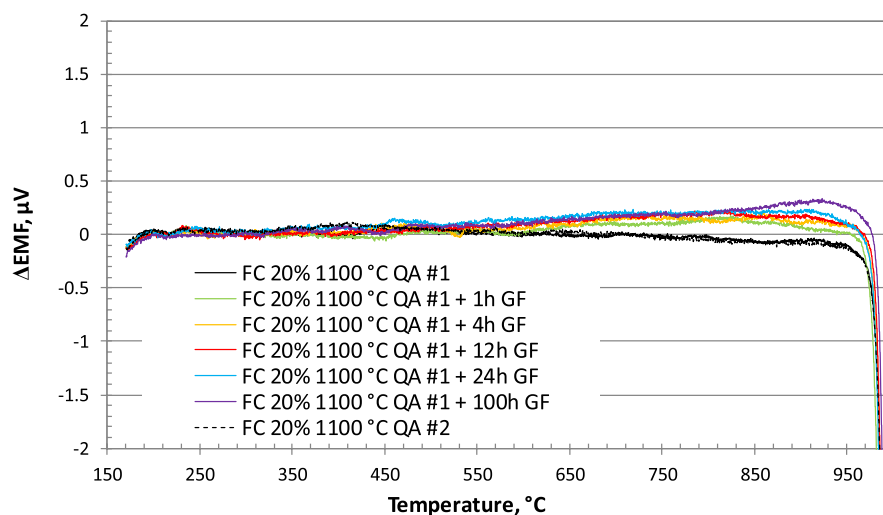
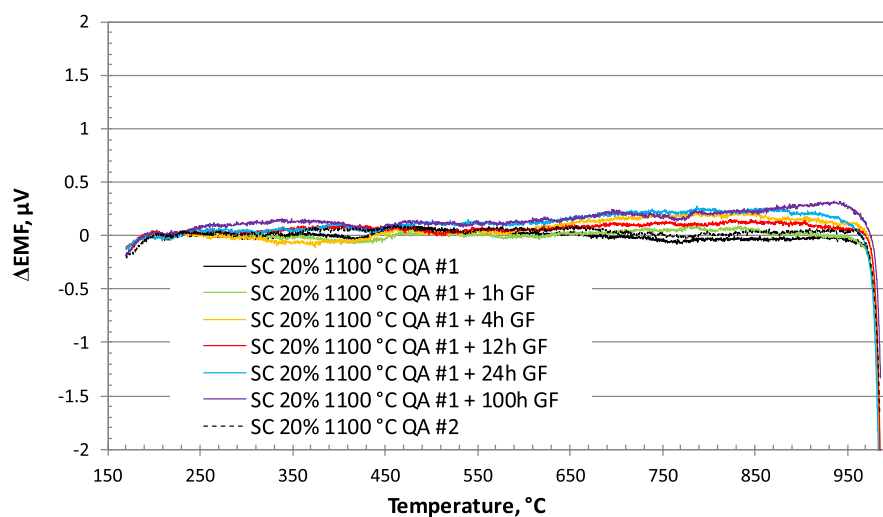**Figure 2.** Deviation in emf of 20TC1 (FC) after gradient furnace aging for 1 h, 4 h, 12 h, 24 h and 100 h.

Figure 3. Deviation in emf of 20TC1 (SC) after gradient furnace aging for 1 h, 4 h, 12 h, 24 h and 100 h.
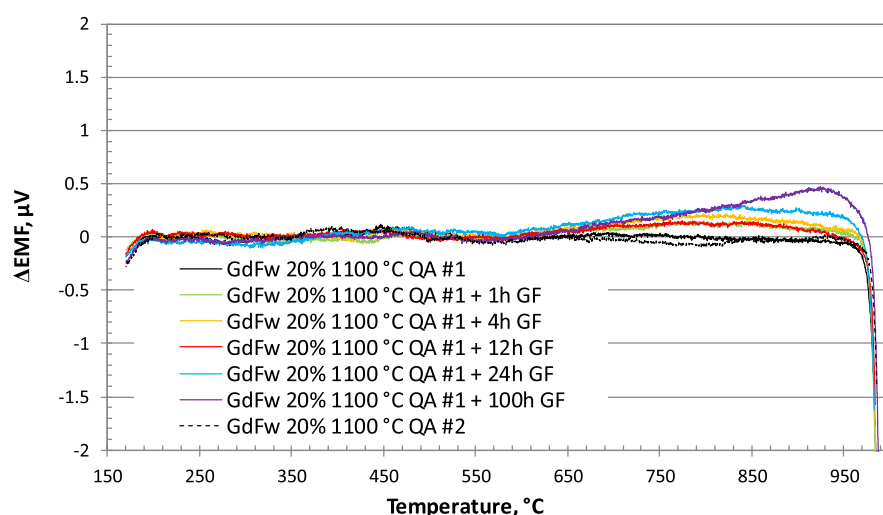

Figure 4. Deviation in emf of 20TC1 (GdFw) after gradient furnace aging for 1 h, 4 h, 12 h, 24 h and 100 h.
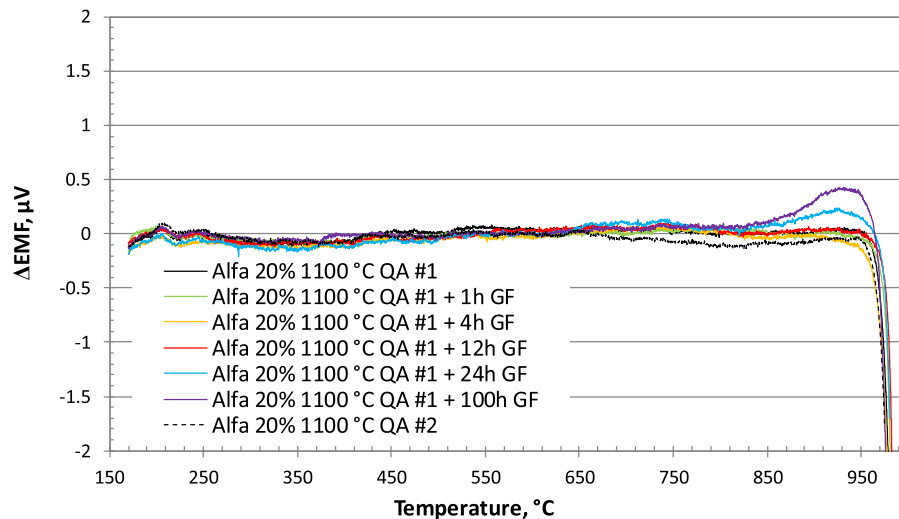
Figure 5. Deviation in emf of 20TC2 (Alfa) after gradient furnace aging for 1 h, 4 h, 12 h, 24 h and 100 h.
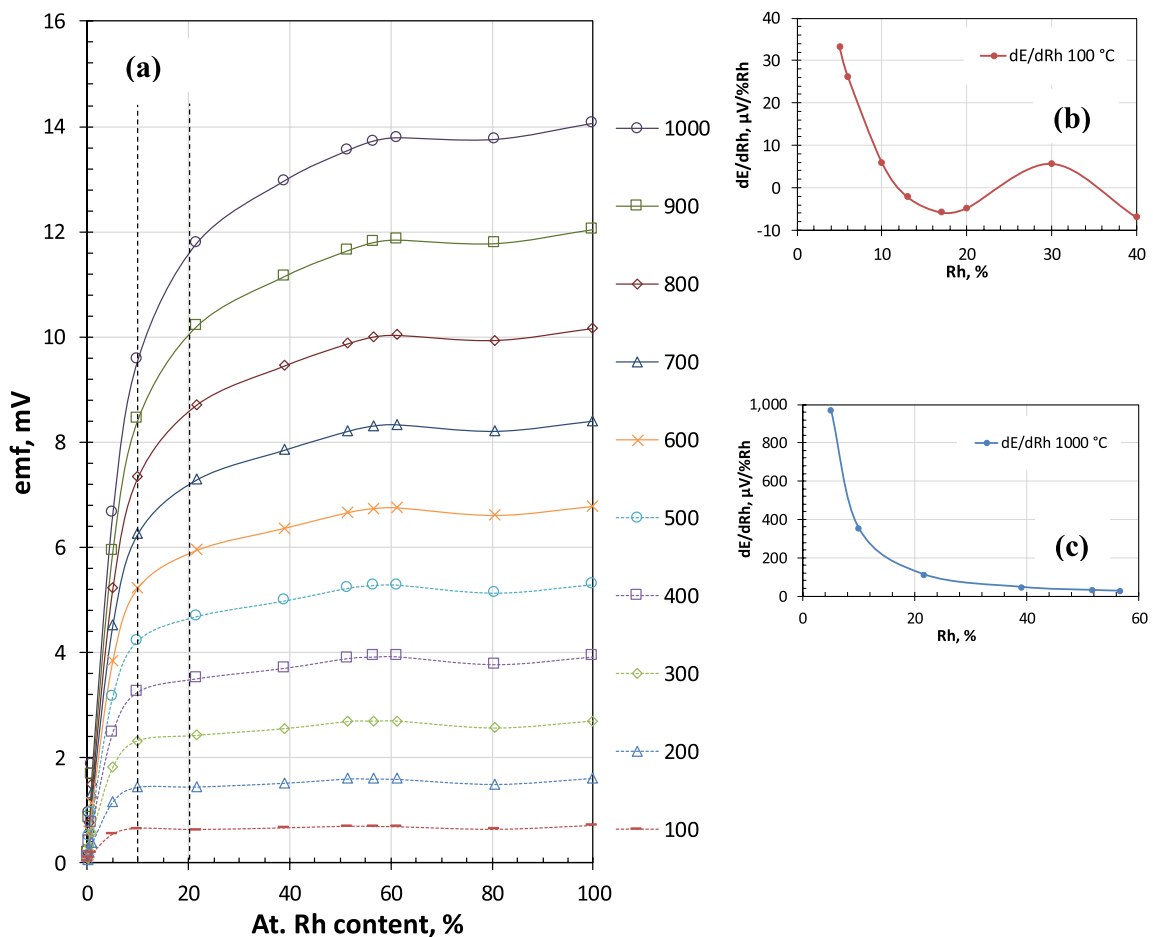

Figure 6. (a) Rh concentration versus emf at selected temperatures [4]. (b) Sensitivity of emf to changes in Rh at 100 °C. (c) Sensitivity of emf to changes in Rh at 1000 °C.

increase in emf, whereas above this temperature a decrease in emf will occur. This Rh sensitivity effect is illustrated in figures 2–5, where we see a small increase in emf for the region exposed to temperatures over 600 °C (when scanned at 100 °C). So, although the scanning results, *prima-facie*, suggest these changes will lead to an increase in emf during normal use at higher temperatures, they will in fact more likely cause

a decrease. This counterintuitive result is due to the temperatures at which rhodium oxide forms, between approximately 600 °C and 1000 °C. At these temperatures, any lowering of the Rh concentration will lead to a reduction in emf.

To better illustrate the effect of changing Rh content on a potential Pt-x%Rh thermocouple, figures 6(b) and (c) are provided. These plots were derived from analytical functions

Table 2. Salt-bath temperature and emf measurements.

Salt, °C (SC)	SC (emf, µV)	Salt, °C (FC)	FC (emf, µV)	Salt, °C (GdFw)	GdFw (emf, µV)	Salt, °C (Alfa)	Alfa (emf, µV)
199.939	1442.264	199.939	1442.838	199.938	1439.534	199.930	1439.718
249.964	1910.293	249.966	1911.383	249.956	1907.908	249.950	1907.521
299.948	2408.796	299.945	2410.783	299.935	2406.045	299.940	2405.991
349.898	2933.886	349.887	2935.950	349.890	2931.193	349.892	2930.904
399.834	3483.188	399.834	3485.323	399.830	3480.431	399.827	3479.807
449.819	4054.997	449.822	4057.405	449.816	4052.393	449.846	4052.000
499.874	4648.426	499.829	4650.482	499.895	4646.265	499.850	4645.302

FC: Franco Corradi, SC: Sigmund Cohn, GdFw: Good Fellow, Alfa: Alfa Aesar.

Table 3. Fixed-point emf measurements.

Fixed-point (temperature, °C)	SC (emf, µV)	FC (emf, µV)	GdFw (emf, µV)	Alfa (emf, µV)	Mean (emf, µV)	Std. dev. (µV)
Ag (961.78)	11 027.42	11 023.31	11 031.18	11 027.69	11 027.40	3.22
Al (660.323)	6681.63	6683.55	6680.19	6680.44	6681.45	1.53
Zn (419.527)	3703.95	3707.60	3701.07	3702.10	3703.68	2.87
Sn (231.928)	1736.17	1739.03	1733.60	1734.89	1735.92	2.32
In (156.5985)	1063.17	1065.31	1061.35	1062.34	1063.04	1.69

FC: Franco Corradi, SC: Sigmund Cohn, GdFw: Good Fellow, Alfa: Alfa Aesar.

fitted to the data over a narrow range of Rh concentrations seen in figure 6(a). These two plots also show how homogeneity scans made at 100 °C can be quite misleading for the Pt-20%Rh versus Pt thermocouple, when compared to the expected behaviour at 1000 °C. At 100 °C the sensitivity is −4.8 µV/%Rh (Type S, +7 µV/%Rh), whereas at 1000 °C it is +125 µV/%Rh (Type S, +351 µV/%Rh). Therefore, homogeneity scanning the Pt-20%Rh thermocouple is needed for the detection of inhomogeneities caused by rhodium oxidation, but to a lesser extent, anticipating this effect at other temperatures. To further illustrate this point, at 100 °C the sensitivity of the Pt-20%Rh alloy to changes in Rh concentration is 68% of that for the Type S and is of opposite sign, whereas, at 1000 °C the ratio is 37% and is of the same sign. Thus, the effects of this type of inhomogeneity cannot be linearly scaled with temperature. An earlier study [30] showed for Type S the effect on the Seebeck coefficient due to rhodium depletion via rhodium oxidation obeyed a square law relationship, doubling between 100 °C and 900 °C. For the Pt-20%Rh thermocouple the effect of rhodium oxide on the Seebeck coefficient changes sign at ~300 °C. Also, given the oxidation effect is only 37% of a typical Type S at 1000 °C we should expect the scans at 100 °C to overestimate the effects of rhodium oxidation.

The insensitivity of the Pt-20%Rh versus Pt thermocouple to thermal history is a highly desirable property, as it avoids many of the problems that degrade Types S and R. Other clear benefits include a reduced reliance on regular annealing to maintain accuracy, the availability of good quality Pt and Pt-20%Rh thermoelements, the cost of quality wire is comparable to reference grade Type S and R wires, immunity to thermally induced mechanical fatigue (a known problem for Pt–Pd and Au–Pt thermocouples) and reduced sensitivity to supplier dependent variations in Rh content. Burns and Gallagher [31] provide good data on the sensitivity of both the Pt-6%Rh and

Pt-30%Rh thermoelements (Type B) to minor changes in Rh content. Therefore, the Pt-20%Rh thermocouple, free from ordering and less susceptible to rhodium depletion effects than the traditional Type S, ought to be capable of greater accuracies through improved stability, when compared to Types R and S.

3.3. Salt-bath measurements between 200 °C and 500 °C and fixed-point measurements between indium and silver

Salt-bath measurements were made in a Hart 6055 high-temperature salt-bath at nominal 50 °C intervals between 200 °C and 500 °C for each of the four thermocouples. The results of these measurements are shown in table 2.

Fixed-point (FP) measurements of the four thermocouples were made on the freeze plateau of each of the ITS-90 fixed points between In and Ag. Table 3 gives the emf values, from which it can be seen the standard deviation from the mean is generally less than about ~3 µV (0.25 °C) at any given FP.

Using the salt-bath and fixed-point data in tables 2 and 3, a tentative reference function can be derived between 0 °C and the silver point (962 °C). This was achieved using a least-squares fit through the four sets of 12 data points. Both weighted and unweighted fits were made on these data points based on standard uncertainties in both temperature and emf. The inclusion of weighting had a negligible effect on the fitting coefficients so was omitted. The minimum number of coefficients needed to generate the polynomial was found to be five, not including the zeroth order coefficient, which must be equal to zero to ensure the function passes through zero at 0 °C. The behaviour is described by a polynomial having the form,

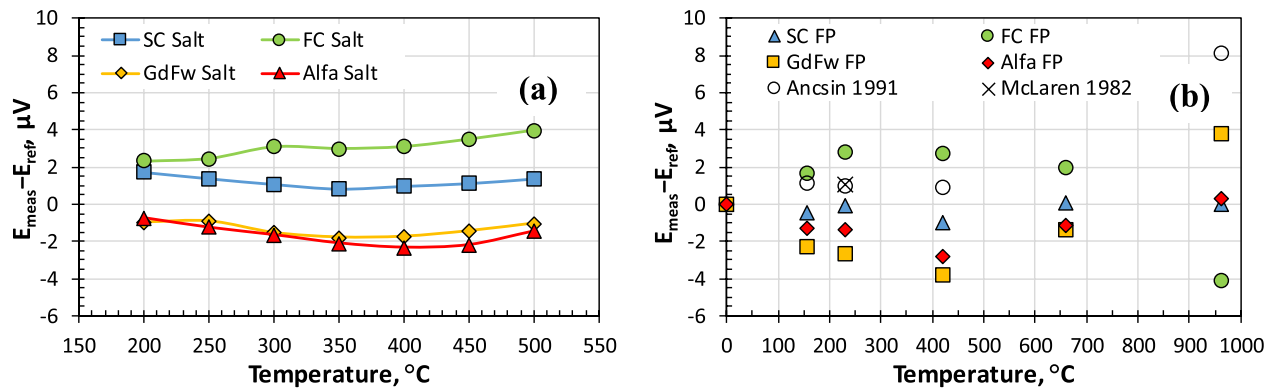$$E = a_1 T + a_2 T^2 + a_3 T^3 + a_4 T^4 + a_5 T^5. \qquad (2)$$

Figure 7. Deviation in emf of four Pt·20%Rh versus Pt thermocouples from a 5th order polynomial reference function for salt bath (a) and fixed-point measurements (b) between 0 °C and 962 °C.
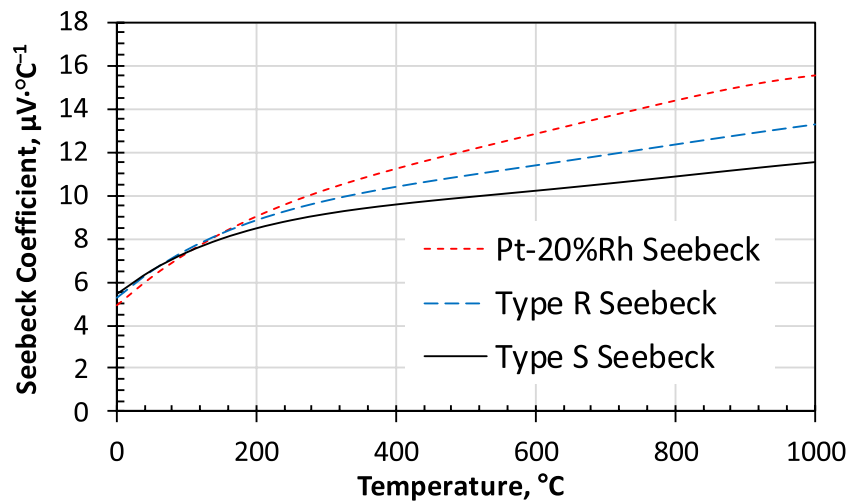

Figure 8. Seebeck coefficient curves for Types R, S and Pt-20%Rh thermocouples.

The coefficients to six significant figures were found to be:

$$a_1 : \quad +4.917\,57$$

$$a_2 : \quad +1.424\,79 \times 10^{-02}$$

$$a_3 : \quad -1.650\,88 \times 10^{-05}$$

$$a_4 : \quad +1.316\,35 \times 10^{-08}$$

$$a_5 : \quad -4.201\,88 \times 10^{-12}.$$

With this polynomial, the residuals were randomly distributed within ± 4 μV of the reference function. A higher-order polynomial was not able to reduce this scatter further, while a lower order polynomial caused a non-random scatter pattern to appear in the residuals.

Using the reference function, the deviation for each thermocouple was plotted as $E_{meas} - E_{ref}$ and is shown in figures 7(a) (salt-bath) and (b) (fixed-points). Also, shown in figure 7(b) is a value given by McLaren [6] at the Sn point and FP values given by Ancsin [32] at In, Sn, Zn, and Ag. The salt-bath measurements revealed the maximum hysteresis was less than 30 mK for all four thermocouples after cycling between 200 °C and 500 °C over 24 h. Similar measurements made with Type S thermocouples resulted in hysteresis of between

Table 4. Uncertainty budget for a typical Pt·20%Rh versus Pt thermocouple calibration after 100 h at ~950 °C.

Component	Uncertainty type	Distribution type	u, μV
Inhomogeneity[a]	B	Rectangular	0.364
DVM noise	A	Normal	0.020
DVM accuracy	A	Rectangular	0.050
DVM drift	B	Normal	0.100
Electronic ice-point stability	A	Normal	0.764
Ext. leads	B	Rectangular	0.108
Immersion	B	Normal	0.270
Interpolation errors	A	Normal	0.601
Total standard uncertainty			1.084
Total expanded uncertainty ($k = 2$)			2.168

[a] If the inhomogeneity is assumed to scale linearly with temperature [30, 37], then, μT (μV) = emf$_T$[emf$_{p\text{-}p}$/(emf$_{T\text{scan}}$ − emf$_{T\text{amb}}$)]/$\sqrt{12}$, where emf$_{p\text{-}p}$ is the peak-to-peak emf observed during a homogeneity scan following 100 h exposure at 950 °C, emf$_{T\text{scan}}$ is the average emf at the scanning temperature (~100 °C), emf$_{T\text{amb}}$ is the emf when at the ambient laboratory temperature (~20 °C) and emf$_T$ is the typical emf at the calibration temperature, T (962 °C).

100 mK and 200 mK. The hysteresis value is the maximum difference in emf between the ramp up and the ramp down in
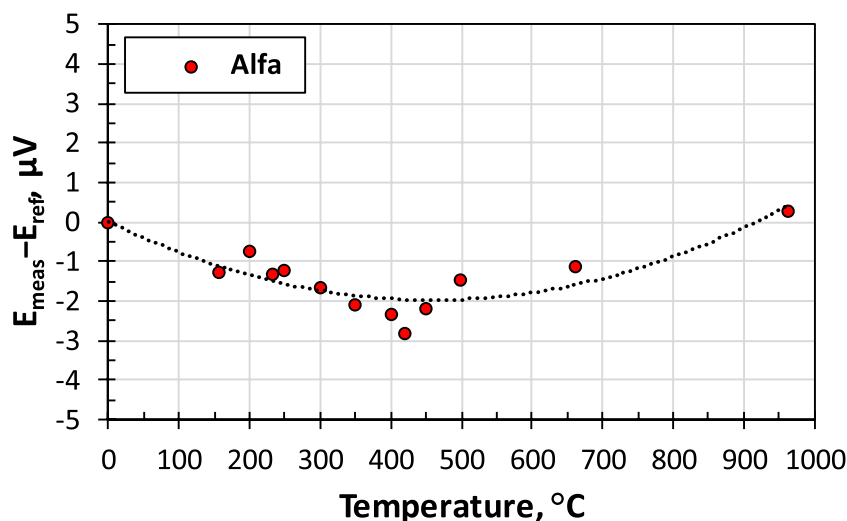
Figure 9. Second-order calibration curve applied to salt bath and fixed-point measurements when employing reference function equation (2).

temperature. This data supports the results given in figures 2–5, which show temperatures below the Ag FP have a minimal effect on the stability of the Pt-20%Rh versus Pt thermocouple and that ordering is not occurring or is insignificant. The salt-bath results also demonstrate why emf values from the other two studies are very close to those obtained here, as there are no apparent Seebeck changes caused by crystallographic ordering effects. Therefore, any variation in the initial anneal given to the wires, beyond a that required to remove cold-working, will have little effect on subsequent measurements.

A further performance benefit in using the Pt-20%Rh thermocouple is it's higher emf above 200 °C when compared to Types R and S; by 1000 °C the emf is almost 20% greater. Figure 8 shows the difference in Seebeck coefficient for the three thermocouple types. The higher signal may be of importance for industrial applications, where the signal-to-noise ratio can be an important factor in determining accuracy.

The problems associated with Types S and R stem from ordering and oxidation related drift, which are absent or minimal in the Pt-20%Rh versus Pt thermocouple. Good examples of this drift for several other Pt–Rh alloys (5%, 10%, 13%, 20%, 30% and 40% Rh) at the Sn and Cu FPs can be found in McLaren's work [6]. In good agreement with the results presented here, McLaren also found the Pt-20%Rh to be the most stable of all the Pt–Rh alloys tested.

It has long been known the initial anneal state for Type R and S thermocouples has a significant impact on the measured emf during calibration at the various fixed-points [6]. However, the effects of disparate annealing treatments were not well understood or quantified at the time the ITS-90 reference functions were generated. These functions were assembled from aggregated data provided by a small number of participants [33–35], up to the gold-point (1064 °C). Each of the participating laboratories could choose their own wire producer and initial anneal state, which varied greatly. For these reasons, the results contained a high level of scatter, leading to a poorly determined reference function, often contributing

to artefacts in the correction functions applied during calibration [36]. Over the past two decades a great deal of research on the metallurgical and chemical changes that occur with temperature in most of the Pt-x%Rh alloys has been made [1, 2, 7, 22, 25], leading to a better understanding of how the initial annealing will affect calibration.

A basic uncertainty budget is given in table 4 to suggest an expected worst-case calibration uncertainty ($k = 2$) after 100 h of use at 950 °C, where no prior annealing was used before calibration. The only component in this table that is poorly defined is the inhomogeneity, for the reasons discussed in section 3.2. Although this component is usually the largest for most thermocouple calibrations, its effect is small here, given the remarkable stability of the 20%Rh alloy when exposed to temperatures below 1100 °C. Since the inhomogeneity term is small the uncertainty budget is now dominated by the uncertainty in the electronic ice-point and interpolation errors. It should be noted that the inhomogeneity term can be roughly halved using an 1100 °C anneal prior to calibration. The total expanded uncertainty of 2.17 μV at 962 °C can be equated to a temperature uncertainty of about 180 mK, using an average Seebeck coefficient of 12 μV·°C^{-1} at ~500 °C. Greater accuracy of ~100 mK ($k = 2$) could be had by replacing the electronic ice-point with a water triple-point cell or real ice-point. This value is comparable to an uncertainty achievable using a Pt/Pd thermocouple. Because reversible temperature induced changes are far smaller than occur in Type S or R, this uncertainty value is not expected to be greater than 140 mK, even after 100 h of use at 1000 °C.

For all four thermocouples, it was found a second order polynomial was sufficient to fit the deviations from the reference function (equation (2)), $E_{meas} - E_{ref}$. Figure 9 shows an example calibration curve for 20TC2 (Alfa). Although, this method is not strictly valid as the reference function was derived from data using the same set of thermocouples, it does provide some indication of the expected behaviour of other Pt-20%Rh versus Pt thermocouples, given the thermoelements in each case were sourced from different suppliers.

The standard deviation in interpolation errors ranged from 0.405 μV to 0.807 μV when fitted, from which an average value of 0.601 μV was used in the uncertainty budget in table 4.

Although fixed point immersion tests are not usually an ideal way of quantifying the magnitude of thermocouple inhomogeneity [23], for the Pt-20%Pt/Rh thermocouple it does provide some limited information, given its unusual emf response to small changes in Rh content with temperature. Immersion tests at each of the FPs indicated the variation in signal over a depth change of 100 mm was no more than 0.2 μV (~20 mK) for any of the four thermocouples tested. Homogeneity scanning (at 100 °C) of these thermocouples after exposure to the Al FP revealed a small and uniform increase in emf for the 400 mm region of the thermocouple subjected to temperatures over 600 °C within the furnace. The increase in emf is consistent with that expected from rhodium oxidation, as seen in figures 2–5 for 1–2 h exposure at approximately 600 °C. Scanning of each thermocouple after exposure to the Ag FP showed a small rhodium oxide peak had formed at approximately 450 mm from the hot junction. This behaviour is also consistent with the formation of rhodium oxide in the furnace temperature gradient region between 600 °C to 900 °C and comparable to that seen in figures 2–5, which have peaks around 800 °C after 1–2 h.

4. Conclusions

This study has shown the potential of the Pt-20%Rh versus Pt thermocouple as a practical replacement for not only the standard Type S and R Pt–Rh thermocouples, but also possibly the Pt–Pd thermocouple for $T < 1100$ °C. Although the Pt-20%Rh versus Pt thermocouple is not intended for high-accuracy use above 1100 °C, this temperature range is still of great importance for many industrial and second-tier laboratories. Using the reference function provided, accuracies of approximately ±0.5 °C appear achievable up to the silver point with minimal effort. With the addition of calibration, the accuracy can be improved to better than ±0.1 °C and the calibration curve need not be more complicated than a second-order polynomial.

Desirably the Pt-20%Rh versus Pt thermocouple appears to be intrinsically stable. It does not suffer from changes in emf caused by crystallographic ordering effects, and rhodium oxidation only causes minor changes in emf due to rhodium depletion effects. As with all Pt–Rh alloys, the rhodium oxide is reversible using an 1100 °C anneal. However, as the effect of the rhodium oxide is so small, this makes reannealing necessary only after more than 100 h of use at temperatures over 800 °C, and only then for the most demanding of applications. Other benefits include a comparable use, assembly and cost to existing Type R and S thermocouples, and it avoids many of the problems associated with the pure metal thermocouples, such as Pt–Pd and Au–Pt, both of which are prone to fatigue breakages and both require hard-to-source high-purity wires. The Pt-20%Rh versus Pt thermocouple may also be of use to laboratories not reliant on a reference function.

Further investigation is needed using larger numbers of samples from different manufacturers and possibly multiple samples from the same supplier, perhaps from different batches of wire. To extend the reference function further, data is also needed from higher-temperature fixed-points, for example Cu and Co–C. These undertakings would require input from other national metrology institutes.

ORCID iDs

E Webster ⬡ https://orcid.org/0000-0002-1788-5904

References

[1] Webster E S 2015 *Int. J. Thermophys.* **36** 1909–24
[2] Webster E S and Edler F 2016 *Int. J. Thermophys.* **38** 1–14
[3] Jahan F and Ballico M 2007 *Int. J. Thermophys.* **28** 1832–42
[4] Caldwell F R 1933 *Bur. Stand. J. Res.* **10** 373–80
[5] Acken J S 1934 *J. Res. Natl Bur. Stand.* **12** 249–58
[6] McLaren E H and Murdock E G 1982 *Temperature, its Measurement and Control in Science and Industry* vol 5, part 2, ed J F Schooley (College Park, MD: American Institute of Physics) pp 953–75
[7] Edler F and Ederer P 2013 *Temperature, its Measurement and Control in Science and Industry* vol 8, part 1, ed C W Meyer (AIP) pp 532–7
[8] Pearce J V *et al* 2015 *Meas. Sci. Technol.* **26** 10
[9] Pearce J 2016 *Johnson Matthey Technol. Rev.* **60** 238–42
[10] Pearce J V, Greenen A D, Smith A and Elliott C J 2017 *Int. J. Thermophys.* **38** 1–12
[11] Roeser W F and Lonberger S T 1958 *NBS* **590** 233–55
[12] Zysk E D 1962 *Temperature, its Measurement and Control in Science and Industry* vol 3, part 2, ed C M Herzfeld (Instrument Society of America) pp 81–134
[13] Kinzie P 1973 *Thermocouple Temperature Measurements* 1st edn (New York: Wiley)
[14] Metcalfe A G 1950 *Br. J. Appl. Phys.* **1** 256–8
[15] Sojka J, Vodárek V, Sobotka J and Dubský M 1991 *J. Less Common Met.* **171** 41–50
[16] Freeman R J 1962 *Temperature, its Measurement and Control in Science and Industry* vol 3, part 2, ed C M Herzfeld (Instrument Society of America) pp 201–20
[17] Selman G L 1972 *Temperature, its Measurement and Control in Science and Industry* vol 4, part 3, ed H H Plumb (College Park, MD: American Institute of Physics) pp 1833–40
[18] Rhys D W 1969 *Metal. Rev.* **14** 47–60
[19] Walker B E, Ewing C T and Miller R R 1962 *Rev. Sci. Instrum.* **33** 1029–40
[20] McLaren E H and Murdock E G 1972 *Temperature, its Measurement and Control in Science and Industry* vol 4, part 3, ed H H Plumb (College Park, MD: American Institute of Physics) pp 1543–60
[21] Bentley R E 1998 *Measurement* **23** 35–46
[22] Bentley R E 1998 *Theory and Practice of Thermoelectric Thermometry* 1st edn (Berlin: Springer)
[23] Webster E S and White D R 2015 *Metrologia* **52** 130–44
[24] Webster E S, White D R and Edgar H 2014 *Int. J. Thermophys.* **36** 444–66
[25] Jahan F and Ballico M 2010 *Int. J. Thermophys.* **31** 1544–53
[26] Li T, Marquis E A, Bagot P A J, Tsang S C and Smith G D W 2011 *Catal. Today* **175** 552–7

[27] Rubel M, Pszonicka M, Ebel M F, Jablonski A and Palczewska W 1986 *J. Less Common Met.* **125** 7–24
[28] Webster E S 2016 *Int. J. Thermophys.* **38** 1–14
[29] Bentley R E 1989 *J. Phys. D: Appl. Phys.* **22** 1902–7
[30] Webster E S, Mason R S, Greenen A and Pearce J 2015 *Int. J. Thermophys.* **36** 2922–39
[31] Burns G W and Gallagher J S 1968 *Precision Measurement and Calibration: Selected NBS Papers on Temperature* vol 2 pp 290–306
[32] Ancsin J 1991 *Metrologia* **28** 339–47
[33] Burns G W, Strouse G F, Liu B M, Mangum B W, Croarkin M C, Guthrie W F and Chattle M 1992 *Temperature, its Measurement and Control in Science and Industry* vol 6, part 1, ed J F Schooley (College Park, MD: American Institute of Physics) pp 559–64
[34] Burns G W *et al* 1992 *Temperature, its Measurement and Control in Science and Industry* vol 6, part 1, ed J F Schooley (College Park, MD: American Institute of Physics) pp 537–40
[35] Burns G W *et al* 1992 *Temperature, its Measurement and Control in Science and Industry* vol 6, part 1, ed J F Schooley (College Park, MD: American Institute of Physics) pp 541–6
[36] Bentley R E 1998 *Metrologia* **35** 41–7
[37] Jahan F and Ballico M 2003 *Temperature, its Measurement and Control in Science and Industry* vol 7, part 1, ed D C Ripple (AIP) pp 469–74